Journal of Beijing Institute of Technology, 2021, Vol. 30, No. 3

A New Image Segmentation Method Based on Fractional-Varying-Order Differential

Yanshan Zhang, Yuru Tian✉

Abstract: In order to solve the problem of image segmentation with intensity inhomogeneity, a new partial differential equation image segmentation model based on fractional-varying-order differential is proposed. This model introduces an adaptive coefficient to set disparate differential order intervals for pixel with different gray values and use fractional-varying-order differential to process the input image combined with the CV model, then use a variety of image segmentation evaluation indicators, such as true positive (TP) rate, false positive (FP) rate, precision (P), Jaccard similarity (JS) rate, and Dice coefficient (DC) rate to measure the pros and cons of our model. The experimental results show that our method is improved on the original basis, which is more conducive to us to obtain more image details and obtain better segmentation results.

Keywords: fractional-varying-order differential; image segmentation; partial differential equation

1 Introduction

The most difficult problem of image segmentation is segmenting intensity inhomogeneity images. At present, researchers have proposed many methods of image segmentation to solve this problem, such as fuzzy clustering [1], semantic segmentation [2], partial differential equation [3], wavelet theory [4] and etc. Among them the partial differential equation as an important branch of basic mathematics, which has formed the theoretical system and the numerical method, has accumulated rich research achievements, and shows strong vitality. The basic idea of the image segmentation method based on partial differential equations is that, on the continuous mathematical model of the image, the image contour changes according to a specified PDE, and the solution of PDE is the desired processing result. The commonly used modeling method is to establish the energy functional and obtain the Euler-Lagrange equation through the variational method. The most typical representative of the partial differential equation method used for image processing is the famous geodesic active contour model [5], which is derived from the snake model [6] and defines a gradient-based edge detector function. Because of the local limitation, this models are sensitive to noise and have difficulty in detecting weak boundary. T F Chan, and L A Vese [7] proposed the CV model, which uses the global information of the image to perform curve evolution. It has a better segmentation effect for targets whose boundaries are not determined by gradients or weak boundaries. However, the intensities within the area of foreground and background always maintain constant because of their assumption, so it does not work well for the intensity inhomogeneity images. To overcome this defect, many methods have been proposed to overcome the difficulty of segmenting intensity

Manuscript received May 24, 2021; revised Jul. 25, 2021; accepted Aug. 30, 2021. The associate editor coordinating the review of this manuscript was Dr. Hongmei Zhu. This work was supported by the Key Research Project of the Henan Provincial Higher Education (No.20A510011).

Yanshan Zhang is with the School of Intelligent Engineering, Zhengzhou University of Aeronautics, Zhengzhou 450046, China.

Yuru Tian is with the College of Computer Science and Technology, China University of Petroleum, Qingdao 266555, China.

✉ Corresponding author. Email: s20070037@s.upc.edu.cn

DOI: 10.15918/j.jbit1004-0579.2021.028

inhomogeneity images. For example, Vese, Chan[8] and Tsai et al.[9] replaced the piece-wise constant intensity by piece-wise smooth intensity to propose a piece-wise smooth (PS) models by minimizing the MS functional[10]. These models have certain capability of handling the intensity inhomogeneity, but they are computationally expensive and the segmentation accuracy is limited. Li et al. proposed a LBF model by incorporating a kernel function to define local binary fitting energy in a variational formulation but it is greatly affected by the initial contour[11]. Then he proposed the LIC model[12] which based on bias field estimation and local intensity clustering property, then proposed a distance regularization which eliminates the need for reinitialization and avoids its induced numerical errors[13].

In recent years, scholars at home and abroad have discovered that fractional differential equations, as an important branch of partial differential equations, play a special role in signal singularity detection and extraction. It can improve the high-frequency components of the signal and retain the low-frequency components of the signal non-linearly. In particular, fractional differential can automatically handle topological changes, which is usually impossible for traditional parametric models. Therefore, it has been applied to the research of image processing by contemporary researchers. Cuesta[14] proposed fractional order linear integral differential equations, which interpolated heat equations and wave equations using the Riemann-Liouville fractional derivative. Mathieu[15] used fractional derivatives to detect image edges. Ren[16] proposed a new adaptive active contour model based on fractional order differentiation for processing images with non-uniform intensity. Chen et al.[17] proposed an adaptive weighted active contour model, which integrates image gradient, local environment and global information into a frame, which better solves the problem of uneven image segmentation. Lv et al.[18] and others used fractional order differentiation in the LBF model to solve the problem that the LBF model is too dependent on the initial contour when processing images.

In this paper, we present a new partial differential equation image segmentation model based on fractional-varying-order differential. First, we calculate the order interval based on the value of the acquired image gradient. On the basis of the original calculation order formula, we introduced an adaptive coefficient to set disparate differential order intervals for pixels with different gray values, which is more conducive to us to obtain more image details. Then according to the obtained order matrix, we use the Fourier domain fractional differential to perform disparate differential order differentiation processing on different positions of the image. Finally, we combined the CV model to segment the image and achieved good results. We also used true positive (TP) rate, false positive (FP) rate, precision (P), Jaccard similarity (JS) rate, and Dice coefficient (DC) rate to measure the pros and cons of the image segmentation results.

The remainder of this paper is organized as follows. In Section 2, we present a brief introduction of several related works. We describe the proposed image segmentation model in details in Section 3. Section 4 presents the experimental results and comparisons on real and synthetic images. Finally, conclusion and outlook for the future are drawn in Section 5.

2 Related Models and Background

2.1 CV Model

This model is to utilize regional mean gray values to decide the contour and divide the image into the targets and background.

Let Ω be the image domain, $\boldsymbol{I}(x,y) : \Omega \to R$ is a given image function, where x, y represent horizontal and vertical coordinates of pixels respectively, and $\boldsymbol{I}(x,y)$ denotes the intensity at a point (x,y). This model is formulated by minimizing the following energy functional:

$$
\begin{aligned}
&E^{\mathrm{CV}}(\boldsymbol{C}, c_1, c_2) = \\
&\lambda_1 \int_{\mathrm{inside}(\boldsymbol{C})} |\boldsymbol{I}(x,y) - c_1|^2 \boldsymbol{H}(\boldsymbol{\phi})x,y))\mathrm{d}x\mathrm{d}y + \\
&\lambda_2 \int_{\mathrm{outside}(\boldsymbol{C})} |\boldsymbol{I}(x,y) - c_2| \, (1 - \boldsymbol{H})\boldsymbol{\phi}(x,y)))\mathrm{d}x\mathrm{d}y + \\
&\mu \int_{\Omega} |\nabla \boldsymbol{H}(\boldsymbol{\phi}(x,y))|\mathrm{d}x\mathrm{d}y + \nu \int_{\Omega} \boldsymbol{H}(\boldsymbol{\phi}(x,y))\mathrm{d}x\mathrm{d}y
\end{aligned} \tag{1}
$$

where λ_1, λ_2 are fixable parameters, $\mathrm{inside}(\boldsymbol{C})$ and $\mathrm{outside}(\boldsymbol{C})$ represent the region inside and outside of the contour $\boldsymbol{C}$, c_1 and c_2 are the mean gray value of the inside or outside region respectively, $\boldsymbol{\phi}(x,y)$ is the level set function and:

$$
\begin{cases}
\boldsymbol{C} = \{(x,y) \in \Omega : \boldsymbol{\phi}(x,y) = 0\} \\
\mathrm{inside}(\boldsymbol{C}) = \{(x,y) \in \Omega : \boldsymbol{\phi}(x,y) > 0\} \\
\mathrm{outside}(\boldsymbol{C}) = \{(x,y) \in \Omega : \boldsymbol{\phi}(x,y) < 0\}
\end{cases} \tag{2}
$$

$H(\cdot)$ is the Heaviside function. Notation $\delta(\cdot)$ indicates the Dirac function and it is defined as the derivative of the Heaviside function $H(\cdot)$

$$
H(z) = \begin{cases} 1, & z \geqslant 0 \\ 0, & z < 0 \end{cases} \tag{3}
$$

$$
\delta(z) = \frac{\mathrm{d}}{\mathrm{d}z} H(z) = \begin{cases} 0, & z \neq 0 \\ \infty, & z = 0 \end{cases} \tag{4}
$$

By minimizing (1), we can obtain c_1 and c_2

$$
\begin{aligned}
c_1 &= \frac{\int_{\Omega} \boldsymbol{I}(x,y)\boldsymbol{H}(\boldsymbol{\phi}(x,y))\mathrm{d}x\mathrm{d}y}{\int_{\Omega} \boldsymbol{H}(\boldsymbol{\phi}(x,y))\mathrm{d}x\mathrm{d}y} \\
c_2 &= \frac{\int_{\Omega} \boldsymbol{I}(x,y)(1 - \boldsymbol{H}(\boldsymbol{\phi}(x,y)))\mathrm{d}x\mathrm{d}y}{\int_{\Omega} (1 - \boldsymbol{H}(\boldsymbol{\phi}(x,y)))\mathrm{d}x\mathrm{d}y}
\end{aligned} \tag{5}
$$

By introducing a length term $\int \boldsymbol{\delta}(\boldsymbol{\phi}(x,y))|\nabla \boldsymbol{\phi}(x,y)| \cdot \mathrm{d}x\mathrm{d}y$ (where ∇ represents the gradient operator) and an area term $\int_{\Omega} \boldsymbol{H}(\boldsymbol{\phi}(x,y))\mathrm{d}x\mathrm{d}y$, which are used to regularize the contour, then minimizing these terms together, we can obtain the following variational formulation:

$$
\frac{\partial \boldsymbol{\phi}}{\partial t} = \delta(\boldsymbol{\phi}) \left[\mu \mathrm{div}\left(\frac{\nabla \boldsymbol{\phi}}{|\nabla \boldsymbol{\phi}|} \right) - \nu - \lambda_1 (\boldsymbol{I} - c_1)^2 + \lambda_2 (\boldsymbol{I} - c_2)^2 \right] \tag{6}
$$

where parameters $\mu \geqslant 0, \nu \geqslant 0$. μ is a scaling parameter, it controls the smoothness of zero level set. If it is small enough, small objects are likely to be extracted, if it is large enough, big objects are likely to be detected. ν increases the propagation speed.

In order to compute the partial differential equation in (6), discontinuous functions $\boldsymbol{H}(\boldsymbol{\phi})$ and $\boldsymbol{\delta}(\boldsymbol{\phi})$ need to be approximated by regularized version $\boldsymbol{H}_{\varepsilon}(\boldsymbol{\phi})$, $\boldsymbol{\delta}_{\varepsilon}(\boldsymbol{\phi})$. In general, the regularized Heaviside function and Dirac function are selected as

$$
\begin{cases}
H_{\varepsilon}(z) = \dfrac{1}{2}\left(1 + \dfrac{2}{\pi}\arctan\left(\dfrac{\boldsymbol{z}}{\varepsilon}\right)\right) \\
\boldsymbol{\delta}_{\varepsilon}(z) = \dfrac{1}{\pi} \dfrac{\varepsilon}{\varepsilon^2 + z^2}, z \in R
\end{cases} \tag{7}
$$

where R represents the set of real number and ε is a small value in the denominator to avoid the singularities. ε is also a predefined parameter for control the speed of the function $\boldsymbol{H}_{\varepsilon}(\boldsymbol{\phi})$ rising from 0 to 1. CV model has good performance in detection of objects whose boundaries are not necessarily defined by gradient or with weak boundaries. However, it generally fails to segment images with intensity inhomogeneity.

2.2 Fourier Domain Fractional Order Differentiation

For a given function of a single variable $f(t)$, it Fourier transform is defined as

$$
F(\omega) = \int_R f(t)\mathrm{e}^{-\mathrm{j}\omega t}\mathrm{d}t \tag{8}
$$

According to the differential property of Fourier transform, the equivalent formulation of the αth-order differential in the Fourier domain is

$$
F(f^{\alpha}(t)) = (\mathrm{j}\omega)^{\alpha} F(\omega) \tag{9}
$$

where α the can be any positive real number. Thus, the fractional order differentiation expression of the function $f(t)$ in frequency domain is defined as

$$
D^{\alpha} f(t) = F^{-1}((\mathrm{j}\omega)^{\alpha} F(\omega)) \tag{10}
$$

where D is the differential operator and F^{-1} is the inverse Fourier transform operator. Thus the fractional order partial differentiation of the two dimensional function $g(x,y)$ can be defined as

$$
\begin{cases}
D_x^{\alpha} g(x,y) = F^{-1}(\mathrm{j}\omega_1)^{\alpha} G(\omega_1, \omega_2) \\
D_y^{\alpha} g(x,y) = F^{-1}(\mathrm{j}\omega_2)^{\alpha} G(\omega_1, \omega_2)
\end{cases} \tag{11}
$$

According to the translation property of the

two-dimension DFT, the center difference schemes of the first order derivative in the Fourier domain can be defined as

$$\begin{cases} D_x^{\alpha} g(x,y) = \\ F^{-1}(1-\exp(-2\pi \mathrm{j}\omega_1/m)^{\alpha}\exp(\pi \mathrm{j}\omega_1/m)G(\omega_1,\omega_2) \\ D_y^{\alpha} g(x,y) = \\ F^{-1}(1-\exp(-2\pi \mathrm{j}\omega_2/m)^{\alpha}\exp(\pi \mathrm{j}\omega_2/m)G(\omega_1,\omega_2) \end{cases} \tag{12}$$

2.3 Fractional-Varying-Order Differential

The fractional-varying-order differential was first proposed and used for image denoising by Zhang et al.[19]. They defined: $\boldsymbol{D}_{\alpha}$ is αth ($\alpha \in R^{+}$) fractional differential operator, $\boldsymbol{u}(x,y) = [\boldsymbol{u}_{ij}(x,y)]_{n\times m}$ is a $n \times m$ image matrix. Then they used matrix operations to make the fractional order differential with disparate order in the matrix act on the corresponding pixels of the image matrix at the same time

$$\boldsymbol{D_A} = \begin{pmatrix} D_{a_{11}} & D_{a_{11}} & \cdots & D_{a_{11}} \\ D_{a_{21}} & D_{a_{22}} & \cdots & D_{a_{2m}} \\ \vdots & \vdots & \ddots & \vdots \\ D_{a_{n1}} & D_{a_{n2}} & \cdots & D_{a_{nm}} \end{pmatrix} \tag{13}$$

$$\boldsymbol{D_A u}(x,y) = \begin{pmatrix} D_{a_{11}}u_{11}(x,y) & D_{a_{11}}u_{11}(x,y) & \cdots & D_{a_{11}}u_{11}(x,y) \\ D_{a_{21}}u_{21}(x,y) & D_{a_{22}}u_{22}(x,y) & \cdots & D_{a_{2m}}u_{2m}(x,y) \\ \vdots & \vdots & \ddots & \vdots \\ D_{a_{n1}}u_{n1}(x,y) & D_{a_{n2}}u_{n1}(x,y) & \cdots & D_{a_{nm}}u_{nm}(x,y) \end{pmatrix} \tag{14}$$

They call $\boldsymbol{D_A}$ as fractional-varying-order differential operator, and

$$\begin{aligned} &\boldsymbol{D_A u} = (\boldsymbol{D}_{\boldsymbol{A}x}\boldsymbol{u}, \boldsymbol{D}_{\boldsymbol{A}y}\boldsymbol{u}) \\ &|\boldsymbol{D_A u}| = \sqrt{(\boldsymbol{D}_{\boldsymbol{A}x}\boldsymbol{u})^2 + (\boldsymbol{D}_{\boldsymbol{A}y}\boldsymbol{u})^2} \end{aligned} \tag{15}$$

The value of $\boldsymbol{A}$ is obtained through the image gradient

$$\boldsymbol{A} = 2 \times (|\nabla \boldsymbol{u}(x,y)| + 1)/(|\nabla \boldsymbol{u}(x,y)| + 2) \tag{16}$$

Because the edge information of the image is often at the position where the image gradient changes the most.

3 Our New Model

3.1 Energy Function

We changed the original coefficient 2 into a variable coefficient based on the calculation method of $\boldsymbol{A}$ proposed by Zhang et al., that is,

$$\boldsymbol{A} = a \times (|\nabla \boldsymbol{u}| + 1)/(|\nabla \boldsymbol{u}| + 0.8) \tag{17}$$

where a is adapting weight, we defined

$$a = \begin{cases} 2.0, & 120 \leqslant \text{grayvalue} < 150 \\ 1.0, & \text{grayvalue} \geqslant 150 \\ 0.1, & \text{grayvalue} < 120 \end{cases} \tag{18}$$

The order of fractional differential can be adjusted adaptively according to the local statistical information and structural characteristics of the image, so that it can be satisfied that it has a large differential order at the strong edge of the image, a small differential order at the weak edge and texture of the image, and a very small differential order at the smoothness of the image. In other words, we get the order of the fractional derivative by the gradient of the image. The range of gray value of the image is [0, 255], the range of gradient can be obtained by difference is [0, 255], then the range of $\boldsymbol{A}$ is

$$\boldsymbol{A} = \begin{cases} [2.0,\ 2.5], & 120 \leqslant \text{grayvalue} < 150 \\ [1.0,\ 1.25], & \text{grayvalue} \geqslant 150 \\ [0.100,\ 0.125], & \text{grayvalue} < 120 \end{cases} \tag{19}$$

Based on CV model and fractional-varying-order differential, we propose our new energy functional model. Our proposed model also consist three parts: the first term $\boldsymbol{E^F}$, the length term $\boldsymbol{E^L}$ and the area term $\boldsymbol{E^A}$. We adapt the first term of CV model as our first term in our energy functional and use the adaptive fractional-varying-order because of its unique advantages as described above. The details are given as

$$|\boldsymbol{D^A u}(x,y)| = \sqrt{(\boldsymbol{D}_{\boldsymbol{A}x}\boldsymbol{u}(x,y))^2 + (\boldsymbol{D}_{\boldsymbol{A}y}\boldsymbol{u}(x,y))^2} \tag{20}$$

$$\boldsymbol{I}(x,y) = \boldsymbol{u}(x,y) - |\boldsymbol{D^A u}(x,y)| \tag{21}$$

Finally, the proposed first term is defined as

$$E^F = \lambda_1 \int_{\text{inside}(C)} |\boldsymbol{I}(x,y) - \boldsymbol{c_1}|^2 \boldsymbol{H}(\boldsymbol{\phi}(x,y)) \mathrm{d}x\mathrm{d}y + \lambda_2 \int_{\text{outside}(C)} |\boldsymbol{I}(x,y) - \boldsymbol{c_2}|(1 - \boldsymbol{H}(\boldsymbol{\phi}(x,y))) \mathrm{d}x\mathrm{d}y \tag{22}$$

And the length term and the area term are following the definition in the CV model.

$$E^L = \int_\Omega |\nabla \boldsymbol{H}(\boldsymbol{\phi}(x,y))| \mathrm{d}x\mathrm{d}y = \int_\Omega \delta(\boldsymbol{\phi}(x,y)) |\nabla(\boldsymbol{\phi}(x,y))| \mathrm{d}x\mathrm{d}y \tag{23}$$

$$E^A = \int_\Omega \boldsymbol{H}(\boldsymbol{\phi}(x,y)) \mathrm{d}x\mathrm{d}y \tag{24}$$

So the final energy functional is

$$\begin{aligned} E &= E^F + E^L + E^A = \\ &\lambda_1 \int_{\text{inside}(\boldsymbol{C})} |\boldsymbol{I}(x,y) - \boldsymbol{c}_1|^2 \boldsymbol{H}(\boldsymbol{\phi}(x,y)) \mathrm{d}x\mathrm{d}y + \\ &\lambda_2 \int_{\text{outside}(\boldsymbol{C})} |\boldsymbol{I}(x,y) - \boldsymbol{c}_2|(1 - \boldsymbol{H}(\boldsymbol{\phi}(x,y))) \mathrm{d}x\mathrm{d}y + \\ &\mu \int_\Omega \boldsymbol{\delta}(\boldsymbol{\phi}(x,y)) |\nabla(\boldsymbol{\phi}(x,y))| \mathrm{d}x\mathrm{d}y + \\ &\nu \int_\Omega \boldsymbol{H}(\boldsymbol{\phi}(x,y)) \mathrm{d}x\mathrm{d}y \end{aligned} \tag{25}$$

Then minimizing these terms together, we can obtain the following variational formulation

$$\frac{\partial \boldsymbol{\phi}}{\partial t} = \boldsymbol{\delta}(\boldsymbol{\phi}) \left[\mu \mathrm{div}\left(\frac{\nabla \boldsymbol{\phi}}{|\nabla \boldsymbol{\phi}|} \right) - \nu - \lambda_1 (\boldsymbol{I} - c_1)^2 + \lambda_2 (\boldsymbol{I} - c_2)^2 \right] \tag{26}$$

where ∇ is the gradient operator.

3.2 Implementation and Algorithm

The implementation and algorithm of this model consists of the following steps:

Step 1 Initialize the level set function $\boldsymbol{\phi}$ to a function $\boldsymbol{\phi}_0$. Then, construct the initial contour $\boldsymbol{C}$.

Step 2 Update $\boldsymbol{\phi}_{i,j}^{k+1} = \boldsymbol{\phi}_{i,j}^k + \Delta t \cdot \boldsymbol{A}(u_{ij}^k)$, where $\boldsymbol{A}(u_{ij}^k)$ is the approximation of the right hand side in (26).

Step 3 Update c_1, c_2 by (4).

Step 4 Check if the set number of iterations is reached. If not, return to Step 2.

4 Experimental Results

In this section, we show the results of multiple image segmentation and use true positive (TP) rate, false positive (FP) rate, precision (P), Jaccard similarity (JS) rate, and Dice coefficient (DC) rate to measure the pros and cons of the image segmentation results, which defined by

$$\begin{aligned} \mathrm{DC} &= \frac{2\boldsymbol{N}(\boldsymbol{S}_1 \cap \boldsymbol{S}_2)}{\boldsymbol{N}(\boldsymbol{S}_1) + \boldsymbol{N}(\boldsymbol{S}_2)} \\ \mathrm{TP} &= \frac{|\boldsymbol{S}_1 \cap \boldsymbol{S}_2|}{|\boldsymbol{S}_2|} \\ \mathrm{FP} &= \frac{|\boldsymbol{S}_1 \cap \boldsymbol{S}_2 - \boldsymbol{S}_2|}{|\boldsymbol{S}_2|} \\ \mathrm{P} &= \frac{\mathrm{TP}}{\mathrm{TP} + \mathrm{FP}} \\ \mathrm{JSC} &= \frac{|\boldsymbol{S}_1 \cap \boldsymbol{S}_2|}{|\boldsymbol{S}_1 \cup \boldsymbol{S}_2|} \end{aligned} \tag{27}$$

where S_1 and S_2 represent the output binary image of the segmentation and binary image of the ground truth. The value of ground truth is obtained by selecting the appropriate threshold through the imbinarize function in the MATLAB software. The closer the values of DC,TP,P and JSC are to 1, the values of FP is to 0, the better the segmentation effect. We also compare results of the proposed model with the CV model, and the LIC model to show the advantages of our model. In addition, all the experiments are carried out by Matlab(R2017b) in the Lenovo laptop with Intel(R) Core(TM) i3-4030U CPU @ 1.90GHz processer. The paramenters are set as follows: λ_1=λ_2=1, ν=0, μ=255, Δt=0.1(the time step).

Firstly, we compared the fixed order differential with order 1.5 and order 0.5 with the fractional-varying-order differential we used. As shown in Fig. 1, the first line is the original image, the second line is fractional-varying-order differential, the third line is the fixed order differential of order 1.5, and the fourth line is the fixed order differential of order 0.5. The rapid change of the gray value of the image edge corresponds to the high frequency, that is, the image edge information is hidden in the high frequency signal. The details of the image also belong to the high frequency area, and it is precisely because of the sharp changes in the gray value that the details

appear. Fractional differential can increase the high-frequency components of the signal, thereby increasing the signal size at the edges and details of the image. At the same time, fractional differential can retain the low-frequency components of the signal non-linearly, which is the area where the gray value changes slowly. For an image, the content inside the edge is a low-frequency signal, and the content inside the edge is most of the information of the image, that is, the approximate appearance and outline of the image. Therefore, if we use fractional differential to process the image, the edge detail area and general outline of the image should be clearer. In the experiment, we tested that the image processing effect of the 1.5-order and 0.5-order fixed-order differentials is not very good. This is because for images with uneven gray values, the values of different pixels are very close, and the difference between the pixels will not be seen if the same differential is used for processing. Therefore, we consider using different differential orders for pixels with differ-

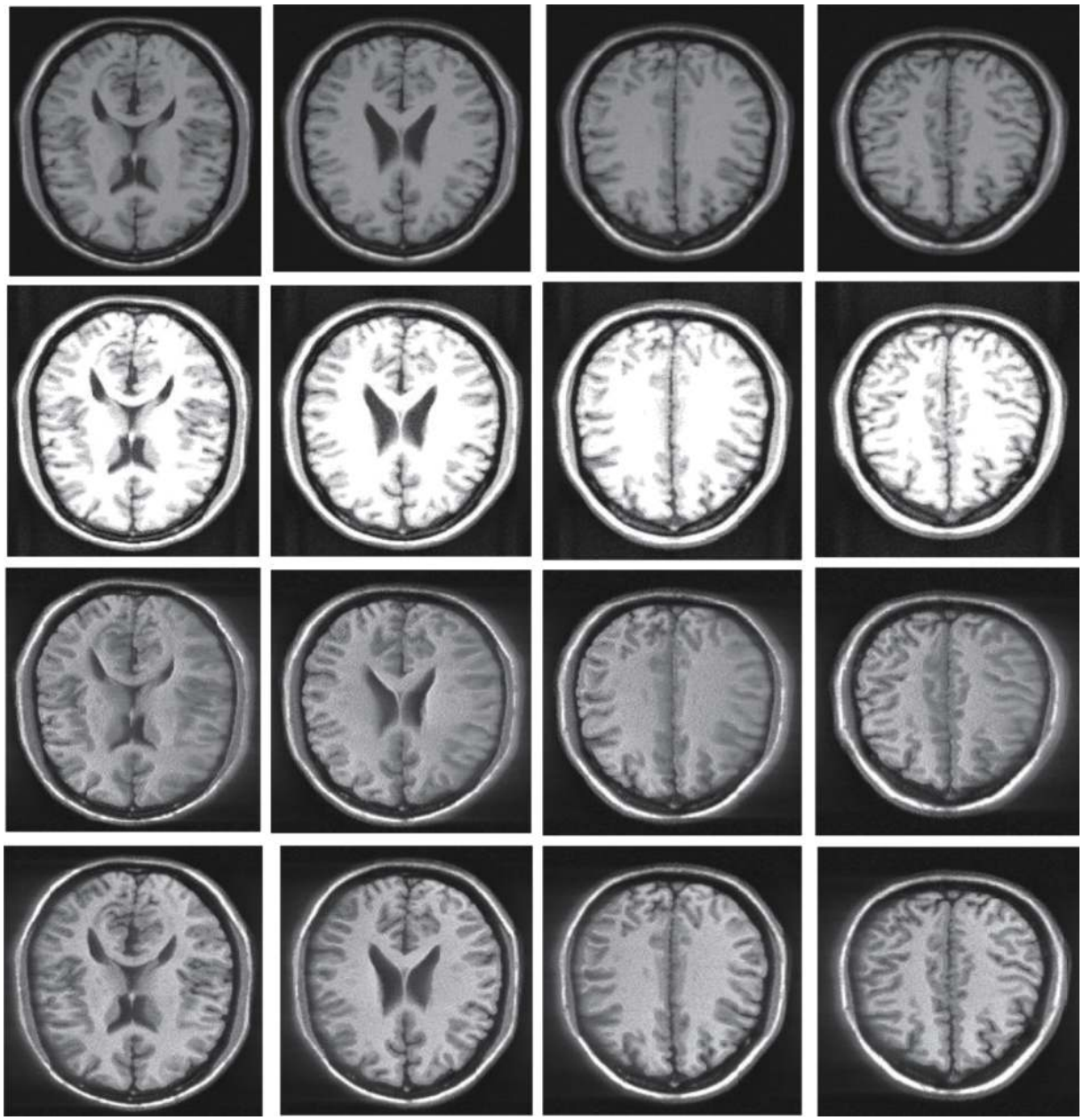

Fig. 1 Comparison of fixed order differential and fractional-varying-order differential

ent gray values to highlight the differences between pixels. It can be clearly seen from the figure that after the varying-order differential processing, the contrast of the image is more obvious, which is more conducive to the task of image segmentation.

Then we applied our method to one image in Fig. 2 with four different initial contours and got the corresponding results. We can see that these different initial contours can finally capture the boundary of the objects from these figures. It confirmed that our model can not be effected by different initial contour. In Tab. 1, we marked the corresponding DC value, TP value, FP value, P value, JCS value to get a more comprehensive understanding of the segmentation results.

Next, in order to prove that our segmentation result is more robust, we used our model to segment the image under the conditions of blur on Fig. 3. We used a defocus blur with a radius of 10 and applied it to the (a) image in Fig. 2. The results are compared with those of other models. Under the condition of blurring, because the edges of the image become less clear, the contours of the three models are slightly reduced in. It can be seen from the values in Tab. 2 that our method performs better in the case of defocus blur compared with other models.

Lastly, we compare our model with the CV mode, the LIC model, and the fixed order differentiation on Figs. 4-6. The order of the fixed order differential is 0.5 order and 1.5 order. The first column of these three images from top to bottom is the original image with the initial contour and the corresponding ground truth. The next few columns in turn are our model, the fixed order is 0.5, the fixed order is 1.5, the CV model and the LIC model. The first line is the segmentation result, and the second line is ground truth of the segmentation result. As shown in Fig. 4, our model can obtain more regions that should be segmented compared with the segmented regions of the CV model and the LIC model. Compared with the two fixed-order differential seg-

(a) (b) (c) (d)

Fig. 2 Different initial contour image segmentation results

Tab. 1 Evaluation index value of different initial contour images

Label	DC	TP	FP	P	JCS	Number of iterations	Average time per iteration
a	0.99383	0.9877	0	1	0.9877	500	0.02512
b	0.99391	0.9879	0	1	0.9879	500	0.02998
c	0.99383	0.9877	0	1	0.9877	500	0.02555
d	0.99390	0.9878	0	1	0.9878	500	0.02549

mentation results, judging from the area contained in the contour in the figure, more areas are segmented when the order is 0.5, however, compared with ground truth, these segmented regions are invalid regions that should not be segmented. Therefore, from the value of the evaluation index (Tab. 3), the region segmented by our model is closer to the ground truth, is numerically better than other models, and the speed of the image segmentation algorithm has not slowed down because of an additional step of fractional-varying-order differential processing compared with CV model.

It can be seen from Fig. 5 that the model with order of 1.5 and order of 0.5 and CV model cannot segment the image with little difference in gray value due to the inappropriate selection of the initial contour. Although the LIC model can segment the image, an extra circle of contours outside the image affects the segmentation effect,

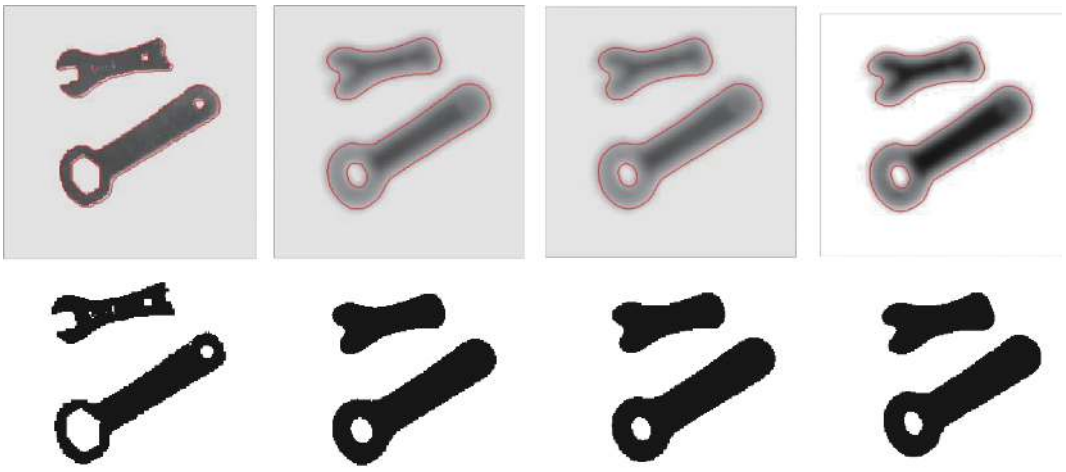

(a) (b) (c) (d)

Fig. 3 Defocus blurred image segmentation results

Tab. 2 Evaluation index value of different defocus blurred images

Label/Model	DC	TP	FP	P	JCS	Number of iterations	Average time per iteration
a/Original	0.9939	0.9878	0	1.0000	0.9878	500	0.02549
b/Our	0.9707	0.9437	6.5701×10^{-4}	0.9993	0.9431	500	0.02134
c/CV	0.9648	0.9324	4.8562×10^{-4}	0.9995	0.9320	500	0.02646
d/LIC	0.9544	0.9127	0	1.0000	0.9127	20	0.17394

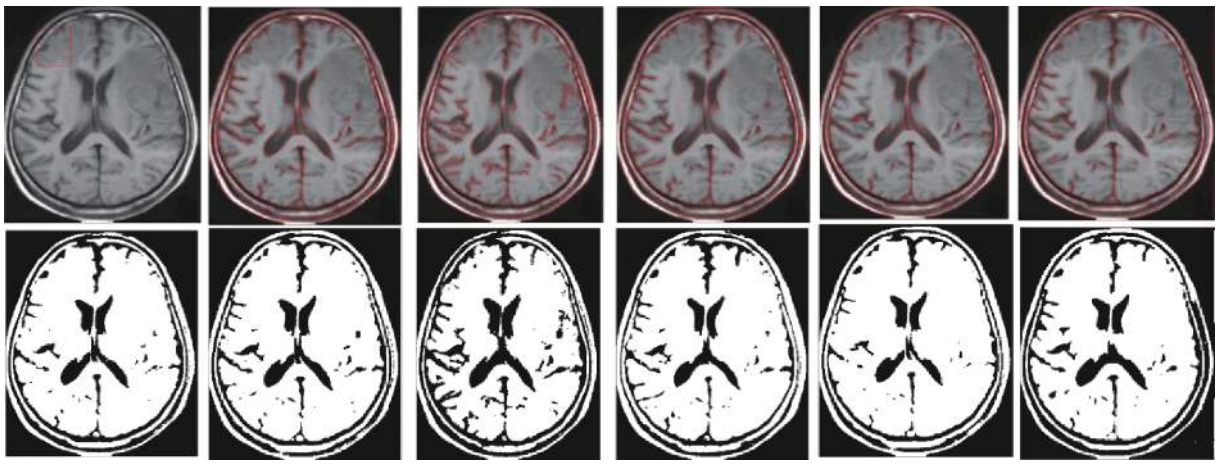

(a) (b) (c) (d) (e) (f)

Fig. 4 Comparison of fixed order, varying-order differentiation and other model segmentation results

so these models do not perform very well from the value of the evaluation index (Tab. 4). Our model can still maintain a good segmentation effect. Fig. 6 and Tab. 5 also prove these.

Tab. 3 Evaluation index value of Fig. 4

Label/Model	DC	TP	FP	P	JCS	Number of iterations	Average time per iteration
b/Our	0.9857	0.9874	0.0160	0.9840	0.9718	500	0.05947
c/0.5 order	0.9479	0.9071	0.0067	0.9927	0.9010	500	0.06958
d/1.5 order	0.9562	0.9708	0.0596	0.9421	0.9161	500	0.06396
e/CV	0.9836	1.0000	0.0334	0.9677	0.9677	500	0.06614
f/LIC	0.9510	0.9210	0.0159	0.9831	0.9066	40	0.26715

Tab. 4 Evaluation index value of Fig. 5

Label/Model	DC	TP	FP	P	JCS	Number of iterations	Average time per iteration
b/Our	0.9862	0.9937	0.0216	0.9787	0.9727	500	0.20926
c/0.5 order	0.6108	1.0000	1.2746	0.4396	0.4396	500	0.20252
d/1.5 order	0.4679	1.0000	2.2748	0.3054	0.3054	500	0.20633
e/CV	0.4577	1.0000	2.3699	0.2967	0.2967	500	0.19347
f/LIC	0.4697	0.8902	1.9005	0.3190	0.3090	40	0.77494

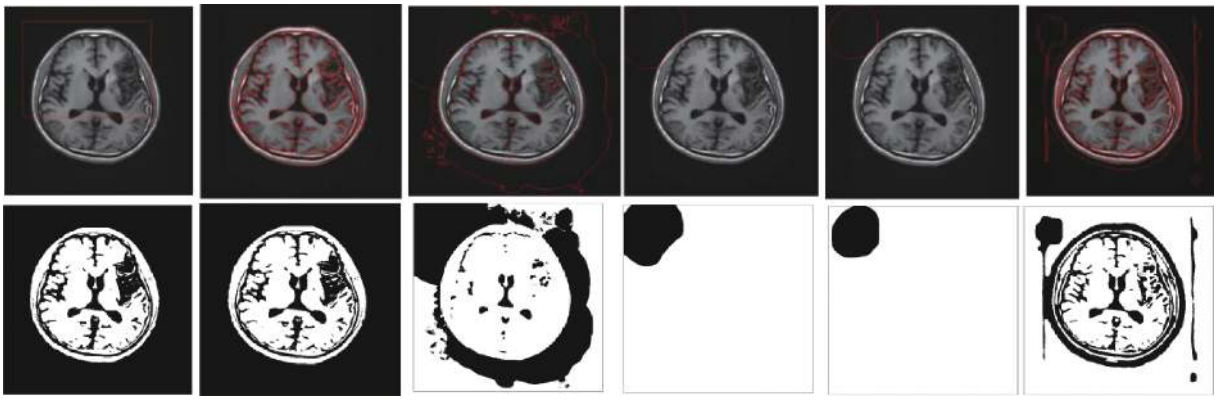

(a) (b) (c) (d) (e) (f)

Fig. 5 Comparison of fixed order, varying-order differentiation and other model segmentation results

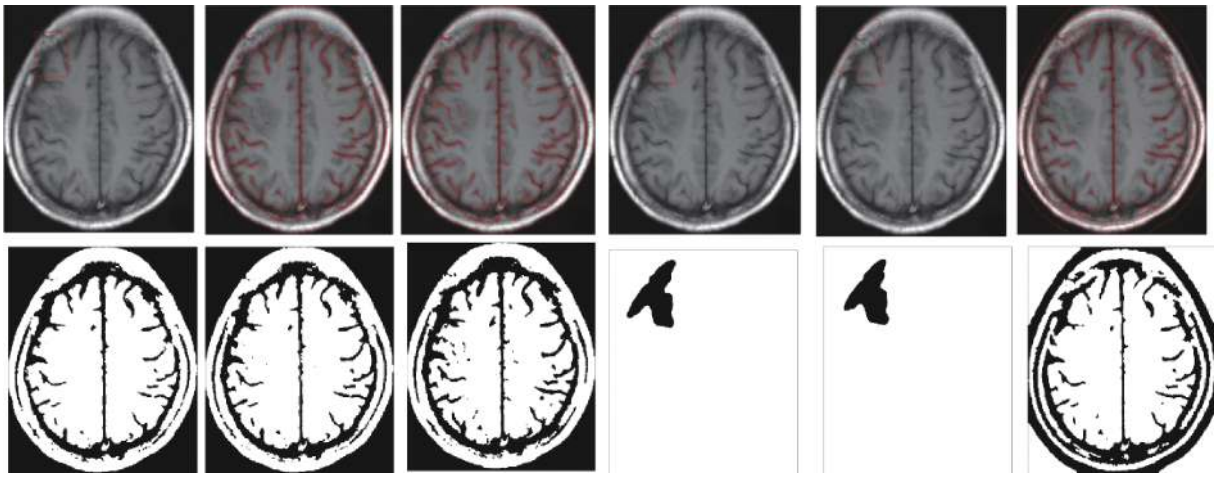

(a) (b) (c) (d) (e) (f)

Fig. 6 Comparison of fixed order-, vary-order differentiation and other model segmentation results

Tab. 5 Evaluation index value of Fig. 6

Label/Mode	DC	TP	FP	P	JCS	Number of iterations	Average time per iteration
b/Our	0.9857	0.9874	0.0160	0.9840	0.9718	500	0.05947
c/0.5 order	0.9479	0.9071	0.0067	0.9927	0.9010	500	0.06958
d/1.5 order	0.9562	0.9708	0.0596	0.9421	0.9161	500	0.06396
e/CV	0.9836	1.0000	0.0334	0.9677	0.9677	500	0.06614
f/LIC	0.9510	0.9210	0.0159	0.9831	0.9066	40	0.26715

5 Conclusion

In this paper, we proposed a new image segmentation model based CV model and apply fractional-varying-order differential to this model. Application of fractional-varying-order differential allows us to have more details about the curve evolution. So our segmentation result is more delicate and closer to the image boundary. We can see our model is much more robust to initialization from the experimental results. From the segmentation results of blurred images, we can see that our model has better performance than the CV model and the LIC model. Compared with other models, it also has a good performance in the segmentation of images with intensity inhomogeneity. In this experiment, we only segment images in the medical field. In our next paper, we will test the segmentation effect of our model on images in other fields, and further discuss the reasons for the effect of the fractional-varying-order differential method on the image. It is hoped that the influence of the fractional-varying-order differential method on the signal can be explained from the other characteristics of the signal. We will also use statistical tests to judge the significance of this method.

References:

[1] A. Bi, W. Ying, and Z. Qian,"Spatial fuzzy clustering and its application for MRI and CT image segmentation," *Journal of Medical Imaging and Health Informatics*, vol. 11, no. 2, pp. 409-412, 2021.

[2] S. Ren, K. He, R. Girshick, and J. Sun,"Faster R-CNN: Towards real-time object detection with region proposal networks," *IEEE Transactions on Pattern Analysis and Machine Intelligence*, vol. 39, no. 6, pp. 1137-1149, 2017.

[3] Y. Wu, M. Li, Q. Zhang, and Y. Liu,"A retinex modulated piecewise constant variational model for image segmentation and bias correction," *Applied Mathematical Modelling*, vol. 54, pp. 697-709, 2018.

[4] J. Gao, B. Wang, Z. Wang, Y. Wang, and F. Kong,"A wavelet transform-based image segmentation method," *Optik*, vol. 208, pp. 164123, 2020.

[5] V. Caselles, R. Kimmel, and G. Sapiro, "Geodesic active contours, " in *Proceedings of IEEE International Conference on Computer Vision*, 1995, pp. 694-699.

[6] M. Kass, A. Witkin, and D. Terzopoulos,"Snakes: Active contour models," *International Journal of Computer Vision*, vol. 1, pp. 321-331, 1988.

[7] T. F. Chan and L. A. Vese,"Active contours without edges," *IEEE Transactions on Image Processing*, vol. 10, no. 2, pp. 266-277, 2001.

[8] T. F. Chan and L. A. Vese,"A multiphase level set framework for image segmentation using the mumford and shah model," *International Journal of Computer Vision*, vol. 50, pp. 271-293, 2002.

[9] A. Tsai, A. Yezzi, and A. S. Willsky,"Curve evolution implementation of the Mumford-Shah functional for image segmentation, denoising, interpolation, and magnification," *IEEE Transactions on Image Processing*, vol. 10, no. 8, pp. 1169-1186, 2001.

[10] M. David and S. Jayant,"Optimal approximations by piecewise smooth functions and associated variational problems," *Communications on Pure and Applied Mathematics*, vol. 42, no. 5, pp. 577-685, 1989.

[11] C. Li, C. Kao, J. C. Gore, and Z. Ding, "Implicit active contours driven by local binary fitting energy, " in *2007 IEEE Conference on Computer Vision and Pattern Recognition*, Minneapolis, America, 2007, pp. 1-7.

[12] C. Li, R. Huang, Z. Ding, J. C. Gatenby, D. N. Metaxas, and J. C. Gore,"A level set method for image segmentation in the presence of intensity inhomogeneities with application to MRI," *IEEE Trans. Image Process.*, vol. 20, pp. 2007-2016, 2011.

[13] C. Li, C. Xu, C. Gui, and M. D. Fox,"Distance regularized level set evolution and its application

to image segmentation," *IEEE Transactions on Image Processing*, vol. 19, no. 12, pp. 3243-3254, 2010.

[14] C. Eduardo and F. Javier, "Image processing by means of a linear integrodifferential equation, " in *Third IASTED International Conference on Visualization, Imaging and Image Processing*, Benalmadena, Spain, 2003, pp. 438-442.

[15] B. Mathieu, P. Melchior, A. Oustaloup, and C. Ceyral,"Fractional differentiation for edge detection," *Signal Processing*, vol. 83, no. 11, pp. 2421-2432, 2003.

[16] Z. Ren,"Adaptive active contour model driven by fractional order fitting energy," *Signal Processing*, vol. 117, pp. 138-150, 2015.

[17] B. Chen, S. Huang, Z. Liang, W. Chen, and B. Pan,"A fractional order derivative based active contour model for inhomogeneous image segmentation," *Applied Mathematical Modelling*, vol. 65, pp. 120-136, 2019.

[18] H. Lv, Z. Wang, S. Fu, C. Zhang, L. Zhai, and X. Liu,"A robust active contour segmentation based on fractional-order differentiation and fuzzy energy," *IEEE Access*, vol. 5, pp. 7753-7761, 2017.

[19] Y. Zhang, F. Zhang, B. Li, and R. Tao,"Fractional domain varying-order differential denoising method," *Optical Engineering*, vol. 53, no. 10, pp. 102102, 2014.

Yanshan Zhang received the Ph.D. degree from Beijing Institute of Technology, Beijing, China, in 2017. Presently, he is a lecturer with School of Intelligent Engineering, Zhengzhou University of Aeronautics. His research interests include digital image processing, fractional calculus, PDE and image processing.

Yuru Tian received the B.S. degree from Zhengzhou University of Aeronautics, Zhengzhou, China, in 2019. She is currently a postgraduate student at China University of Petroleum. Her research interests include digital image processing and knowledge graph.